Journal Pre-proofs

Calcium-looping for thermochemical energy storage in concentrating solar power applications: evaluation of the effect of acoustic perturbation on the fluidized bed carbonation

Federica Raganati, Riccardo Chirone, Paola Ammendola

PII: S1385-8947(19)33073-6
DOI: https://doi.org/10.1016/j.cej.2019.123658
Reference: CEJ 123658

To appear in: *Chemical Engineering Journal*

Received Date: 20 September 2019
Revised Date: 11 November 2019
Accepted Date: 29 November 2019

Please cite this article as: F. Raganati, R. Chirone, P. Ammendola, Calcium-looping for thermochemical energy storage in concentrating solar power applications: evaluation of the effect of acoustic perturbation on the fluidized bed carbonation, *Chemical Engineering Journal* (2019), doi: https://doi.org/10.1016/j.cej.2019.123658

Calcium-looping for thermochemical energy storage in concentrating solar power applications: evaluation of the effect of acoustic perturbation on the fluidized bed carbonation

Federica Raganati, Riccardo Chirone, Paola Ammendola*

Istituto di Ricerche sulla Combustione (IRC) – CNR, Piazzale Tecchio 80, 80125 Naples, Italy

*Corresponding author

Tel.:+39 0817682237; fax:+39 0815936936.

E-mail address: paola.ammendola@irc.cnr.it

Calcium-looping for thermochemical energy storage in concentrating solar power applications: evaluation of the effect of acoustic perturbation on the fluidized bed carbonation

Federica Raganati, Riccardo Chirone, Paola Ammendola *

*Corresponding author

Tel.:+39 0817682237; fax:+39 0815936936.

E-mail address: paola.ammendola@irc.cnr.it

ABSTRACT

In the framework of thermochemical energy storage (TCES) in concentrating solar power (CSP) plants, the calcium-looping (CaL) process, carried out in fluidized bed reactors, is receiving increasing research interest due to the high energy density and the extremely low price, nontoxicity, and wide availability of natural CaO precursors. One of the main open challenges in CaL is represented by finding solutions to the progressive decline in the CaO carbonation conversion with the number of cycles, which is due to the sorbent deactivation caused by sintering and pore pugging. In this framework, the reduction of the CaO particles size has been reported to improve the carbonation conversion and, therefore, the achievable energy density, by maximizing the availability of the sorbent surface exposed to the gaseous phase and hindering the natural loss of CaO mutlicyclic activity. However, the use of fine particles in fluidized bed reactors is challenging due to agglomeration, channeling and plugging phenomena.

In this work, the possibility to use a fine natural limestone (<50μm) for CaL at TCES-CSP conditions in a fluidized bed reactor has been investigated for the first time. In particular, sound-assisted fluidization has been proposed as technique to allow the use of such fine particles in fluidized bed reactors, thus overcoming the strict limitation posed by particle size applicable in ordinary fluidized bed reactors. Ordinary and sound-assisted cyclic CaL tests at CSP-TCES operating conditions have been performed in a lab-scale fluidized bed reactor in order to study the influence of the application of high intensity acoustic fields on the carbonation performances. The effect of sound parameters (SPL and frequency) has also been highlighted.

Keywords: Thermochemical energy storage (TCES); Concentrating solar power (CSP); Fine particles; Calcium looping; Agglomeration; Sound-assisted Fluidization

1. Introduction

The main challenge for a short-term deeper penetration of renewable energy sources, such as solar energy, typically characterized by the intermittency of power production, is represented by energy storage [1–3]. In this framework, thermochemical energy storage (TCES) is one of the most promising technology to achieve high-energy storage efficiency in concentrating solar power (CSP) plants [2]. TCES basically consists of using the high temperatures achievable by CSP to drive an endothermic chemical reaction [1]. The reaction products are stored separately to be employed when needed for carrying out the exothermic reverse reaction, which releases the heat previously used [1].

Among the different alternatives, the calcium-looping (CaL) process, based on the reversible calcination−carbonation of the $CaCO_3$/CaO system, is considered to be one of the most viable candidates due to the high energy density achievable and the extremely low price, nontoxicity, and wide availability of natural CaO precursors such as limestone [1]. Indeed, the carbonation/calcination reaction of CaO, with an equilibrium temperature of 895°C (under a CO_2 partial pressure of 1atm), has a high potential for TCES in the relatively high temperature range attainable in CSP tower plants (roughly between 600 and 1000°C [3]) and would allow also for a high energy storage density (about 3.26 GJm^{-3}) [1]. As regards the reactor configuration, CaL is generally performed in fluidized bed reactors, acting as either carbonator or calcinator [4]. It is noteworthy that the optimum conditions to carry out the CaL process strongly depend on the particular application, thus critically affecting the CaO multicycle performance [5]. In particular, to achieve high overall efficiency for TCES and electricity generation in CSP plants, carbonation would be carried out at high CO_2 partial pressure and high temperature (around or above 800 °C), thus yielding high efficiency thermal to electricity efficiency of the power cycle. On the contrary,

*Corresponding author
Tel.:+39 0817682237; fax:+39 0815936936.
E-mail address: paola.ammendola@irc.cnr.it

calcination could be performed at relatively low temperature (~750 °C) at low CO_2 partial pressure by using a gas easily separable from CO_2, such as superheated steam or helium, thus reducing costs and allowing the use of already available solar receiver [5]. Of course, using He for calcination would require the separation of the He/CO_2 gas mixture exiting from the calciner, that could be carried out relatively easily by means of selective membranes due to the differences in molecular size of helium (similar to H_2) and CO_2 [6]. It should be taken into account that the need also exists to realize a process characterized by free CO_2 emissions. To this aim, the CaL-CSP will be performed according to a closed cycle scheme, as thoroughly discussed by Chacartegui et al. [6]. In this configuration a pure CO_2 stream is fed to the carbonator with a molar rate well above the stoichiometric needs for carbonation. The excess CO_2 leaving the carbonator is used as heat carrier fluid to remove the heat released during carbonation and sent to a gas turbine for power production by means of a CO_2 closed Brayton cycle. Then it is compressed and stored for the successive cycles. Of course, the fact that this scheme is a closed cycle implies that it does not require the plant to be continuously fed by any gas stream, which applies also and especially in the case of helium, which is a very expensive gas [6].

Carbonation of CaO particles occurs in two phases. A first fast carbonation stage is characterized by the sorption of CO_2 on the free surface of the particles and proceeds under mass/heat transfer control [4,7]. The rate of this fast carbonation phase is not just controlled by the kinetics of the chemical reaction itself, but also by the transport of CO_2 and heat to the particles surface [4]. Therefore, carbonation can be strongly hindered by poor gas/solids contact efficiency [4]. Then, after this fast stage, a thin layer of $CaCO_3$ covers the free surface of the sorbent particles and CO_2 sorption turns to be controlled by a much slower phase characterized by the diffusion of CO_2 through the solid $CaCO_3$ layer [8]. In this framework, one of the main drawbacks of the

*Corresponding author
Tel.:+39 0817682237; fax:+39 0815936936.
E-mail address: paola.ammendola@irc.cnr.it

$CaO/CaCO_3$ system, is the progressive decline in the carbonation conversion with the number of cycles, which is due to the CaO deactivation caused by sintering and pore pugging. The loss of CaO carbonation activity has been thoroughly investigated in recent years in the framework of CO_2 capture [9–11] and, more recently, also in the context of TCES applications [12–15], since it is strictly related to the achievable energy density. In particular, several methods have been proposed to hinder the natural loss of CaO multicycle activity, such as hydration [16], thermal activation [17,18], mechanical grinding [15,19] and the use of synthetic Ca-based sorbents with enhanced activity [14,15,20]. Besides these methods, another solution which has been receiving increasing research interest is the use of fine particles due their large surface to volume ratio [12,13]. Indeed, it has been reported that the use of CaO small particles can strongly limit sintering and pore-plugging, thus consequently enhancing the multicyclic CaO conversion at the conditions to be used for TCES [12,13]. In particular, as clearly and thoroughly reported by Benitez-Guerriero et al. [12] and Ortiz et al. [13], the effect of particle size on the multicycle conversion of CaO stems from to the relative thickness of the $CaCO_3$ layer formed on the CaO surface as compared to the size of the pores in the CaO skeleton formed after the fast reaction-controlled stage of the carbonation reaction. In particular, they showed that the carbonate layer can become thicker than 100 nm, whereas, the size of the pores generated in the CaO skeleton is typically lower than 50 nm under operating conditions typical of CaL for TCES-CSP [12,13] (i.e. carbonation at high temperature and CO_2 partial pressure and calcination at low temperature in inert environment), thus leading to significant pore-plugging for relatively large CaO particles [12,13]. Besides, the CaO pores that become plugged by the carbonate layer in the case of coarse particles are more inclined to sinter in the successive calcinations, thus further reducing the CaO surface area available for carbonation [12,13]. In contrast, they showed that fine particles (< 45 μm), characterized by larger surface to volume ratio,

*Corresponding author
Tel.:+39 0817682237; fax:+39 0815936936.
E-mail address: paola.ammendola@irc.cnr.it

can provide the important advantage of reducing the strength of pore-plugging with respect to coarser particles [12,13]. More specifically, the pores of the smaller particles can be fully accessible to the CO_2, which leads to carbonation of the whole available CaO surface, thus limiting the decline of the multicycle CaO conversion at the conditions to be used for TCES-CSP [12,13]. In particular, it has been shown that CaL multicyclic performances exhibited by limestone is strongly hindered for particles larger than 45 μm, having a conversion after 20 cycles, X_{20}, of about 0.18 [12,13]. Whereas, on the contrary, particles smaller than 45 μm can provide remarkably higher and more stable conversion performances (X_{20} = 0.45), thus indicating that particle size does affect CaL under these condition [45]. Moreover, besides the limitation of the natural loss of sorbent activity over repeated cycles, it should be considered that small particle can provide better gas-solid contact efficiency due to the higher surface to volume ratio with respect to coarser particles [21]. More specifically, reducing the size of the sorbent particles can allow to increase the availability of the sorbent surface exposed to the gaseous phase, which is reported to positively affect the fast initial phase of the carbonation reaction (i.e. before the formation of the $CaCO_3$ passivation layer and the switch to the slow diffusion phase) as well as the reaction kinetics does [4]. As a result, the overall conversion and, therefore, the achievable energy density can be enhanced. In spite of the proved potential of fine CaO/$CaCO_3$ particles for TCES-CSP applications, it should be noted that all the results available in literature have been obtained by thermogravimetric analysis [12,13], which is intrinsically unable to address all the issues concerning the gas-solid contact and mass/heat transfer efficiency occurring in a fluidized bed reactor [20].

As a matter of fact, the use of fine particles poses issues concerning their intrinsic difficulty to be fluidized, thus imposing a strict limitation on the size of particles actually utilizable in common fluidized bed reactors [22–24]. Indeed, fine particles, i.e. belonging to the C group of Geldart's

*Corresponding author
Tel.:+39 0817682237; fax:+39 0815936936.
E-mail address: paola.ammendola@irc.cnr.it

classification [25], cannot be fluidized under ordinary conditions since interparticle adhesion forces prevail over hydrodynamic and gravitational forces, thus leading to agglomeration and channeling phenomena [23,26–29], which in turns would remarkably hinder the reaction efficiency due to poor and heterogeneous gas/solid contact and mass/heat transfer. Therefore, the achievement of a smooth fluidization regime, in the case of such fine particles is closely related to the overcoming of interparticle forces and to an efficient break-up of the large aggregates yielded by these forces. To this aim, externally assisted fluidization can be used, thus involving the application of additional forces that can be generated by: mechanical vibration [30,31], magnetic field [32,33], acoustic field [28], electric field [34,35], centrifugal fields [36–39], secondary gas flow via micro-jets [40,41] and pulsation [42–44]. Besides the above-mentioned techniques, another approach is represented by the addition to the bed of foreign flow-conditioning particles, which can be either coarser [45,46] or finer [47,48] than the powder to be fluidized. Among these available techniques, sound-assisted fluidization is recognized to be one of the most promising alternatives, holding also several advantages from a practical point of view [23,28]: i) it is not intrusive, since neither additional equipment nor materials must be inserted in the bed; ii) the powders to be employed do not need to have any special property; iii) the application of acoustic fields is capable of reducing the elutriation of fine particles from a fluidized bed, preventing problems related to down-stream carry-over of fine particles such as clogging of valves; iv) last but not least, this technique is extremely economical and user-friendly, since the extra equipment (signal generator, audio amplifier loudspeaker and oscilloscope) required is very easily available on the market. From the phenomenological point of view, the sound-assisted fluidization can be explained considering that the application of the sound wave causes an oscillatory motion of both gas molecules and solid particle/aggregates [4,49–51]. The entity of this motion depends on the size of particles/clusters:

*Corresponding author
Tel.:+39 0817682237; fax:+39 0815936936.
E-mail address: paola.ammendola@irc.cnr.it

obviously, the sound perturbation affects smaller structures much more than larger ones [52,53]. Therefore, this different response of differently sized aggregates to the sound wave induces a relative motion between them, which is the very reason causing a dynamic break-up mechanism of larger clusters into smaller subclusters, which can be more easily fluidized. More specifically, as proposed by the theoretical cluster/subcluster oscillators model developed by Russo et al. [53], the disruption of clusters into smaller aggregates occurred at the contact points between them, i.e. where the collision energy induced by the acoustic field becomes larger than the interparticle cohesive force. Besides having an effect on the fluid-dynamics of the system, sound waves also induce a number of phenomena taking place at the gas/solids interface, such as acoustic streaming, which has been proved to contribute to the enhancement of mass/heat transfer rates in gas/solids reactors [4]. Even though sound-assisted fluidization has only been tested at lab-scale level and its actual feasibility has not been proved yet at industrial-scale, it can be argued that the scale-up of the process would not be too challenging [49]. In particular, few key aspects should be taken into account. The first issue arises from sound intensity attenuation across the bed height. In particular, for such fine materials and for low frequency sound waves (around 100 Hz), it can be estimated that the SPL is reduced by 10 dB for each 10 cm of bed [49]. So, it would not be possible to use bed higher than 40–50 cm. Accordingly, the only way to scale-up the process is represented by increasing the reactor diameter [49]. However, this diameter increase would lead to another cause of sound intensity attenuation, namely the divergence of the acoustic wave [49]. A feasible technique to avoid spherical spreading loss is to use an array of loudspeakers, which may produce a plane wave if conveniently placed on the cross-sectional area of the column [54,55]. Besides, the use of an array of loudspeakers would also provide a greater reliability for continuous operation, since replacement of one of the loudspeakers can be easily carried out without the interruption of the

*Corresponding author
Tel.:+39 0817682237; fax:+39 0815936936.
E-mail address: paola.ammendola@irc.cnr.it

sound assisted process [49]. With reference to the economic feasibility, clearly the use of fine sorbent particles by means of sound-assisted fluidized bed reactors, as most of the solutions proposed to address and limit the natural loss of CaO multicycle activity (e.g. hydration [16], thermal activation [17,18], mechanical grinding [15,19] and the use of synthetic Ca-based sorbents with enhanced activity [14,15,20]), would implies some additional costs with respect to the standard CaL process. In this framework, some energy cost estimations on sound-assisted CaL are available in a previous work [4]. It has been shown that the additional energy requirement (due to the sound generation) to convert a fixed amount of CO_2/sorbent in the sound-assisted process is greatly outbalanced by the increased energy consumption (due to prolongued heating and pumping) necessary to carry out slower carbonation reactions under ordinary conditions [4]. Of course, these estimations are based on results derived from lab-scale experiments [4]. As far as energy cost is concerned, it must be taken into account that the additional energy requirement for gas heating and pumping in ordinary conditions depends linearly on the gas flow rate whereas the excess of energy needed for sound generation is quite insensitive to it [4]. Thus, it might be envisaged that energy saving derived from sound-assisted conditions would be magnified in real industrial applications, where fluidized beds are operated at gas flow rates much larger than those used in our lab-scale tests [4].

In this work, for the very first time a technological solution, i.e. sound-assisted fluidization, has been proposed to make fine limestone particles actually usable for TCES-CSP applications. In particular, a fine natural limestone (< 50 μm) has been tested for the first time in a lab-scale fluidized bed reactor at CaL TCES-CSP conditions. In particular, sound-assisted fluidization has been applied to promote the fluidizability of such fine particles, thus addressing and overcoming the limitation of particle size than can be used in ordinary fluidized bed reactors. Ordinary and sound-

*Corresponding author
Tel.:+39 0817682237; fax:+39 0815936936.
E-mail address: paola.ammendola@irc.cnr.it

assisted cyclic calcination/carbonation tests at CSP-TCES operating conditions have been performed in order to study the influence of the application of high intensity acoustic fields on the carbonation performances. The effect of sound intensity (SPL) and frequency (f) have been also highlighted.

2. Experimental

2.1 Materials

The sorbent used in this work is a natural limestone from Belchite quarries (Spain) supplied by OMYA. Fresh and cycled (after carbonation/calcination cycles carried out in the fluidized bed apparatus under ordinary and sound-assisted) samples have been characterized as follows:

- The particle size distribution of the sorbent has been obtained by laser diffractometry using a Mastersizer 2000 granulometer (Malvern Instruments), after the dispersion of the powders in water under mechanical agitation of the suspension.
- The morphological features of the sorbent have been highlighted by scanning electron microscopy (SEM) using a Philips XL30 SEM instrument.
- The measurements of specific surface area (SSA) have been performed by means of N_2 adsorption and desorption at 77 K with a QUANTACHROM 1-C analyzer. In particular, the values of SSA have been calculated using the Brunauer–Emmet–Teller (BET) equation.

2.2 Experimental apparatus

All the tests have been carried out at atmospheric pressure in the lab-scale apparatus reported in Fig. 1. It consists of a fluidized bed column made of quartz (40 mm ID and 1500 mm high) and it is equipped with a Pyrex gas distributor plate located at 300 mm from the bottom of the column. The section of the column below the gas distributor, filled with quartz rings, acts as wind-box,

*Corresponding author
Tel.:+39 0817682237; fax:+39 0815936936.
E-mail address: paola.ammendola@irc.cnr.it

maximizing the uniformity of the gas flow entering the fluidized bed. The column is provided with a pressure probe located at the wall, 5 mm above the gas distributor, to measure the pressure drops across the bed.

A heating jacket (Tyco Thermal Controls GmbH) has been used to heat the column up to the desired temperature. In particular, it has been designed to cover, besides the fluidized bed section, also part of the column below the gas distributor, which can, thus, act as a preheating chamber for the fluidizing gas. The temperature inside the fluidized bed is monitored and controlled using a type K thermocouple, with a diameter of 1 mm, connected to a PID controller.

The sound-generation system consists of a digital signal generator, a power audio amplifier rated up to 40 W, and a 8W woofer loudspeaker. The acoustic field is introduced inside the column through a purpose-designed sound waveguide located at the top of the freeboard. Separate high purity N_2 and CO_2 cylinders (99.995% vol.) have been used to prepare the gas feed, using two mass flow controllers (Brooks 8550S) to set and control the inlet flowrates.

The analysis system consists of a continuous analyzer, to monitor the outlet CO_2 concentration by means of an infrared detector (ABB AO2020, URAS 14).

2.3 Preliminary fluid-dynamic characterization

Prior to the CaL tests, the limestone has been previously characterized from the fluid-dynamic point of view performing fluidization tests under both ordinary and sound-assisted conditions. N_2 has been used as fluidizing gas in order to prevent any intensification of the powder cohesiveness due to air moisture. For all the tests 100 g of limestone have been loaded in the fluidization column in order to obtain a bed height of about 15 cm. Pressure drops and bed expansion curves as functions of gas velocity have been measured in fluidization experiments carried out at different temperatures

*Corresponding author
Tel.:+39 0817682237; fax:+39 0815936936.
E-mail address: paola.ammendola@irc.cnr.it

(25 - 850 °C) and using acoustic fields of different intensities (120−150 dB) and frequencies (50−300 Hz). Then, experimental data have been worked out to calculate the main fluidization parameters. In particular, the minimum fluidization velocity (u_{mf}) has been evaluated from pressure drop data and the average size of fluidized particles (d_p) has been evaluated from the experimental values of u_{mf} by using the correlation proposed by Wen and Yu [56].

2.4 Cyclic carbonation/calcination tests

The specific carbonation/calcination conditions used in this work have been selected to simulate a CaL-CSP scheme with calcination occurring at low temperature under helium atmosphere and integrated with a closed CO_2 Brayton cycle for power generation [57].

Pre-treatment: The $CaCO_3$ sample (100 g) is firstly subjected to a pre-calcination step (T = 900 °C) for 2h under N_2 flow (115 NLh^{-1}), corresponding to a superficial gas velocity of 2.5 cm/s, which is about five times larger than the minimum fluidization velocity of the sorbent material, to obtain pure CaO. In particular, this pre-treatment has been carried out under sound-assisted conditions (150dB – 120Hz, which are the best acoustic parameters obtained from the fluid-dynamic characterization) in order to obtain the starting materials under the same operating conditions for all the different tests.

Carbonation/Calcination cycles: After the pre-treatment stage, the sample is subjected to 10 carbonation/calcination cycles, where a cycle consists of a carbonation step followed by a calcination step. The carbonation step is carried out at 850°C using a mixture of 70% CO_2/30% N_2 vol/vol (115 NLh^{-1}) as inlet gas flowrate until the complete saturation of the bed. Then, this is followed by the subsequent calcination stage, which is carried out at 750 °C but switching the inlet gas flowrate (115 NLh^{-1}) to N_2, up to complete decarbonation for regeneration of the sorbent. Carbonation tests have been carried out under both ordinary and sound-assisted fluidization

*Corresponding author
Tel.:+39 0817682237; fax:+39 0815936936.
E-mail address: paola.ammendola@irc.cnr.it

conditions (120 – 150dB/50 – 300Hz); whereas, all the calcination tests have been carried out under sound-assisted fluidization conditions (150dB – 120 Hz). The use of N_2 in the lab-scale rig is an experimental expedient and, of course, no N_2 would be used in the real industrial plant. More specifically, N_2 has been used: during carbonation to create a feeding mixture so that the analysis system, a continuous analyzer equipped with an infrared detector, could detect variations in the CO_2 concentration of the stream leaving the reactor, due to the progress of reaction; during calcination to substitute the expensive helium as inert gas. It is important to underline that the validity of all the results obtained and discussed in the following sections in the framework of a CSP-TCES application hold true and is not affected by the use of N_2 in the experimental tests. In particular, as regards the carbonation reaction, it is widely accepted that the carbonation conversion and multicycle stability of limestone are insensitive to the concentration of CO_2 in the feed [58–61]; i.e. using a 70%/30%vol. CO_2/N_2 stream is the same as using a pure CO_2 stream in terms of CaO conversions and multicycle stability. Likewise, as regards the calcination reaction, N_2, exactly like He, is an inert gas and does not take part actively in the reaction.

By elaborating the curve of CO_2 concentration in the gaseous stream leaving the fluidized bed reactor, the CaO conversion (carbonation conversion, X_{Ca}) has been calculated. In particular, X_{Ca} has been evaluated from the amount of CO_2 reacted with CaO during the carbonation step by integrating the outlet CO_2 concentration profile [62–65]) according to:

$$X_{Ca} = \frac{n^R_{CO_2}}{n_{CaO}} = \frac{\frac{1}{m}\int_0^{t_s}(Q_{CO_{2,in}} - Q_{CO_{2,out}})dt}{n_{CaO}} \quad (1)$$

where n_{CaO} are the moles of CaO present in the sorbent, $n^R_{CO_2}$ are the moles of CO_2 reacted with CaO during the carbonation reaction, m is the mass of CaO in the bed (i.e. the amount of the sample after the pre-calcination step), $Q_{CO2,in}$ and $Q_{CO2,out}$ are to the molar flowrate of CO_2 at the inlet and outlet

*Corresponding author
Tel.:+39 0817682237; fax:+39 0815936936.
E-mail address: paola.ammendola@irc.cnr.it

of the bed, respectively, t_s is the time at which the carbonation conversion is over (i.e. the CO_2 concentration in the outlet stream is equal to the inlet value).

Then, the experimental data of CaO conversion during multiple cycles have been fitted using the semi-empirical equation [11]:

$$\frac{X_N}{X_1} = \frac{X_r}{X_1} + \left(\frac{1}{k(N-1) + \left(1 - \frac{X_r}{X_1}\right)^{-1}} \right) \quad (2)$$

where, X_N is the conversion in cycle N, X_r is the residual conversion, X_1 is the conversion in the first cycle and k is the deactivation rate constant.

3. Results

3.1 Material characterization

Figs. 2a reports the particle size distribution of the limestone; it can be inferred that it is characterized by particles smaller than 50 μm. In particular, it has a Sauter diameter of 4 μm, thus indicating that it belongs to Group C of Geldart's classification [25].

The analysis of the SEM image, reported in Fig. 2b, confirms the natural tendency of the limestone particles to organize themselves in the form of aggregates as large as tens of microns. As a matter of fact, the finer particles stick to other particles leading to agglomerated structures due to the action of strong interparticle forces.

The BET SSA of the fresh limestone is 1.6 m^2 g^{-1}, which is in line with the quite low values typically reported for natural limestones [66,67].

3.2 Preliminary fluid-dynamic characterization

Fig. 3 reports the dimensionless pressure drops ($\Delta P/\Delta P_0$) curves obtained for the limestone at ambient temperature under ordinary and sound-assisted conditions (150 dB–80 Hz), where ΔP is the

*Corresponding author
Tel.:+39 0817682237; fax:+39 0815936936.
E-mail address: paola.ammendola@irc.cnr.it

actual pressure drop across the bed and ΔP_0 is the pressure drop equal to buoyant weight of particles per unit area of bed. For uniform fluidization, the pressure drops are equal to the material weight per unit area (i.e. $\Delta P/\Delta P_0 = 1$), thus indicating that the whole bed is fluidized [28].

The results of the fluid-dynamic characterization show that the fluidization quality is quite a poor under ordinary conditions. Indeed, the pressure drop curve is quite irregular and a proper fluidization regime cannot be reached due to agglomeration and channeling, as typical of cohesive powders [23,28]. In particular, since the interparticle forces begin to predominate over weight and drag forces, the individual particles tend to adhere to one another, thus causing the formation of agglomerates (agglomeration phenomena) that, in turn, lead to channeling and plugging phenomena (i.e. remarkable decrease of the permeability of the particle bed by the interstitial fluid) [23,28].

On the contrary, the pressure drops curve obtained with the assistance of sound is far more regular, from both the qualitative and quantitative point of view. This is due to the continuous break-up mechanism of the large aggregates present inside the bed into smaller fluidizable ones yielded by the acoustic field. In particular, the acoustic perturbation induces the action of external (drag and inertial) forces, which counteract the internal (cohesive) forces [23]. More specifically, as proposed by the theoretical cluster/subcluster oscillators model developed by Russo et al. [53], the disruption of clusters into smaller aggregates occurred at the contact points between them, i.e. where the collision energy induced by the acoustic field becomes larger than the interparticle cohesive force.

The role played by the sound intensity and frequency of the acoustic field has also been evaluated in order to obtain the most effective acoustic conditions. In particular, Fig. 4 report the experimental values of the minimum fluidization velocity, experimentally evaluated from the pressure drops curves, and fluidizing particle size, evaluated from the values of minimum fluidization velocity, as functions of SPL at fixed frequency (120 Hz) and as functions of frequency at fixed SPL (150 dB),

*Corresponding author
Tel.:+39 0817682237; fax:+39 0815936936.
E-mail address: paola.ammendola@irc.cnr.it

respectively. First of all, it is clear that the fluidizing agglomerate size are larger than the nominal size of the powder (i.e. the Sauter diameter obtained from the granulometric distribution). The application of the sound makes it possible to actually achieve a fluidization state of the limestone, but in the form of aggregates rather than original (i.e. the "effective" size of the fluidizing structures is the size of the particle aggregates), undergoing a dynamic break-up and reaggregation mechanism.

With reference to the effect of the sound parameters, SPL has a beneficial effect on the fluidization quality. Indeed, d_p and u_{mf} are always decreased by passing from 120 to 150 dB (Fig. 4a). This evidence is due to the fact that with increasing SPLs more energy is introduced inside the bed, thus making the break-up of larger clusters more and more efficient [23]. This means that, with increasing SPLs, smaller the limestone can be fluidized in the form of smaller aggregates, thus leading to a consequent reduction of the minimum fluidization velocity.

Sound frequency, on the contrary, has a non-monotonic effect on the fluidization quality, i.e. both u_{mf} and d_p exhibit a nonlinear relationship with the sound frequency. Indeed, the curves of u_{mf} and d_p are characterized by a minimum value at 120 Hz, i.e. (Fig. 4b). This behavior is due to the fact that the frequency directly affects the relative motion between clusters and subclusters, which, in turn, promotes the break-up and reaggregation mechanism [23]. In particular, when the frequency is too high, the acoustic field cannot properly propagate inside the bed since the sound absorption coefficient is proportional to the square of sound frequency as sound propagates through the bed of particles [23]. Therefore, most of the acoustic energy is absorbed by the upper part of the bed (being the sound source located at the top of the column), whereas, the bed bottom is reached by a strongly attenuated sound wave, thus failing to efficiently disrupt large agglomerates at the bottom of the bed. As a consequence, the fluidization quality decreases, i.e. u_{mf} increases [23,28]. On the contrary,

*Corresponding author
Tel.:+39 0817682237; fax:+39 0815936936.
E-mail address: paola.ammendola@irc.cnr.it

when the sound frequency is too low, the relative motion between larger and smaller sub-aggregates is practically absent, thus also resulting in poor break-up mechanism and fluidization quality [23].

Figures 5 reports the fluidization curves obtained at different temperatures and u_{mf} and d_p as functions of temperature, respectively. The results obtained show that increasing temperatures lead to increased fluidization difficulty, as confirmed by the pressure drop curves shifting to the right (Fig. 5a). This result cannot be explained on the basis of purely hydrodynamic considerations on the effect of temperature on gas viscosity and density because interparticle forces are also simultaneously active, and they become more and more intense as temperature is increased [23,26,27,68]. As a matter of fact, increasing temperatures lead to the intensification of the interparticle forces, which causes, in turn, the formation of larger fluidizing structures, i.e. higher values of d_p (Figure 5b) [23,26,27] because more and more particles tend to sticks together. As a consequence of the increased size of the fluidizing aggregates u_{mf} is also increased when temperature is increased from 25 to 850 °C. Notably, even though the acoustic field becomes less effective as the temperature is increased, its break-up mechanism is still remarkable as shown in Fig. 6. In particular, agglomeration and channeling phenomena occurring inside the bed are evidently shown in the picture taken during the ordinary fluidization test performed at 850°C (Fig. 6a). On the contrary, the picture taken during the sound-assisted fluidization test carried out at 850°C (Fig. 6b) clearly shows the homogeneity of the fluidization quality achievable when sound is applied.

3.3 Cyclic carbonation/calcination tests

Figure 7a reports the comparison between the CO_2 outlet concentration profiles obtained under ordinary and sound-assisted conditions, which is an indication of the degree of progress of the carbonation reaction. More specifically, CO_2 molecules continuously enter the bed and react with

*Corresponding author
Tel.:+39 0817682237; fax:+39 0815936936.
E-mail address: paola.ammendola@irc.cnr.it

the sorbent, which is loaded in the reactor in a batch mode. Therefore, the reaction goes on until all the available sorbent is carbonated and the CO_2 outlet concentration approaches the feeding value (70%).

It is clear that the application of the acoustic perturbation remarkably enhances the carbonation performances. In particular, under both ordinary and sound-assisted fluidization conditions, the two characteristic phases of the carbonation reaction, i.e. the first fast carbonation stage and the slow diffusion-controlled one, are clearly evidenced by the change of the slope in the CO_2 concentration profile. However, it is also clear that the turning point from one phase to the other occurs much earlier when no acoustic field is applied. Indeed, under ordinary fluidization conditions the carbonation turns to be controlled by diffusion after less than 2 min, as evidenced by the long tail of the CO_2 concentration profile (during this period carbonation slowly occurs after the formation of the carbonate product layer). On the contrary, when sound is applied the duration of the fast carbonation stage is prolonged to about 15min and, as a consequence, the CO_2 concentration profile is characterized by a much shorter tail. As a consequence, the carbonation reaction occurs globally faster under sound-assisted fluidization conditions. Indeed, under sound-assisted fluidization conditions, the reaction is essentially concluded after 20 min, which means that the majority of the sorbent is carbonated during the fast reaction phase. On the contrary, after the same time during the ordinary test the reaction is far to be concluded. In particular, the slow diffusion-controlled part of the reaction is still taking place, as confirmed by the CO_2 outlet concentration being still lower than the inlet value (70%vol.). As a matter of fact, since the turning point between the fast and slow carbonation phases occurs after less than 2 min, the majority of the sorbent is carbonated during the slow diffusion-controlled phase.

*Corresponding author
Tel.:+39 0817682237; fax:+39 0815936936.
E-mail address: paola.ammendola@irc.cnr.it

The explanation of these experimental evidences is due to the fluidization quality being extremely poor and unstable under ordinary conditions; as a matter of fact, the severe agglomeration phenomena strongly reduce the surface of CaO available to the gaseous phase. Then, unable to overcome the cohesiveness of the fine sorbent particles, most of the inlet gas manages to flow across the bed only by finding channels of minimum resistance [9]. Spreading across the bed, these channels allow for a by-pass of an appreciable volume of gas (as clearly shown in Fig. 6a), thus hampering the quality of gas–solid contact and in turn the carbonation reaction efficiency. Indeed, the agglomeration phenomena affect both the gaseous (CO_2) and solid ($CaCO_3$) reactants taking part to the carbonation reactions. As for the gaseous side, agglomeration is the reason why only a small fraction of the inlet CO_2 takes part to the carbonation reaction, since most of it by-passes the bed through the channels (i.e. the reaction mainly takes place on the sorbent particles placed at the wall of the gas channels). Accordingly, most of the gaseous reactant, CO_2, exit the bed without reacting with CaO [4,20]. As for the solid side, agglomeration also remarkably reduces the actual availability of sorbent surface to the carbonation reaction. Due to agglomeration, a large portion of the sorbent surface is completely precluded to the fluid phase. Therefore, the general result of the sorbent agglomeration is a continuous and sudden increase of the CO_2 outlet concentration. Indeed, the more easily available CaO surface is soon covered with the carbonate layer, thus CO_2 can continue to react with CaO only by diffusing through this layer (i.e. quick shift to the slow diffusion-controlled stage).

On the contrary, the application of the sound makes it possible to hinder the agglomeration phenomena, evidently shown in Fig. 6b, thus enhancing the fluidization quality and providing better gas–solid contact and mass transfer coefficients [69,70]. Accordingly, channels are disrupted (Fig. 6b) and, as for the gaseous side, more CO_2 can properly permeate the sorbent bed and take part to

*Corresponding author
Tel.:+39 0817682237; fax:+39 0815936936.
E-mail address: paola.ammendola@irc.cnr.it

the carbonation reaction. Likewise for the solid side, a larger surface of the sorbent can actually come into direct contact with the fluidizing gas and react with the CO_2 [4,70]. The application of the sound makes it possible to maximize the exploitation of the sorbent reactivity. Indeed, even though fluidized in the form of aggregates, these fluidizing structures are not static but dynamic. They undergo a continuous mechanism of break-up and reaggregation, which means that the sorbent surface exposed to the gaseous phase is continuously renewed.

From the analysis of Fig. 7a it is also noteworthy that the differences between the ordinary and sound-assisted tests are more evident in the initial stage of the reaction, i.e. during the fast stage of the carbonation reaction. As a matter of fact, the acoustic perturbation has a stronger effect in the initial kinetically controlled stage of the carbonation reaction. Indeed, during this phase, in which the carbonation conversion is ascribable to the sorption of CO_2 on the free surface of the sorbent particles, the capability of the sound to increase the gas-solid contact efficiency [4], i.e. the enhancement of the sorbent surface availability, can provide a strong beneficial impact. After the fast phase of the carbonation reaction, i.e. once the layer of $CaCO_3$ begins to cover the free surface of the particles, the reaction turns to be controlled by the diffusion of CO_2 through the solid $CaCO_3$ layer [4]. Therefore, even though the effect of the sound on the fluid-dynamics of the system is still active, its impact on the carbonation reaction is less important since it is strictly related to diffusion mechanisms rather than to the availability of sorbent surface and, therefore, to the quality of the gas-solid contact.

As a further confirmation of these considerations on the positive effect yielded by the sound on the CaL performances, a specific test has been carried out, in which the sound was switched on at a certain time. In particular, the test has been started under ordinary conditions and only at a time t* the sound has been turned on (Fig. 7a). This test emphasizes, even more significantly, how the

*Corresponding author
Tel.:+39 0817682237; fax:+39 0815936936.
E-mail address: paola.ammendola@irc.cnr.it

sound can affect the extent and evolution of the carbonation reaction. The non-monotonic trend obtained for the CO_2 outlet concentration can be explained considering that until t*, the system (sorbent + CO_2) shows the same behavior as that obtained for the ordinary test (i.e. for $t < t^*$ the CO_2 outlet concentration profile is the same as that obtained under ordinary conditions). Then, when the sound has been switched on at t*, the CO_2 concentration suddenly drops down before rising up again, but following now the typical trend of the sound-assisted test. This is due to the fact that the amount of sorbent surface, which is precluded to the fluid during the fast carbonation stage under ordinary conditions (due to the severe agglomeration phenomena), suddenly becomes available. As a consequence, this renewal of sorbent reactivity (due to the sorbent surface renewal yielded by the sound) causes the CO_2 concentration to drop down. This result is the clear proof of the actual ability of the sound to provide a better exploitation of the sorbent surface.

Figures 7b reports the results obtained in terms of carbonation conversion as a function of time. Consistently with the observed enhancement of the carbonation reaction (Fig. 7a), the carbonation conversion is also increased under sound-assisted conditions due to the better exploitation of both the gaseous (CO_2, which can properly permeate the sorbent without by-passing it unused due to agglomeration) and solid (CaO, which can come into direct contact with the CO_2 and does not remain unreacted) reactants.

Fig. 8, reporting the carbonation conversion as a function of cycle number and deactivation fit curve obtained under ordinary and sound-assisted-fluidization conditions, shows that the deactivation rate is reduced and the residual conversion is increased when sound is applied. Clearly, as widely documented [8], the CaO reactivity decreases with increasing the number of carbonation/calcination cycles due to the progressive reduction of surface area as a result of the sintering of nascent CaO particles during the calcination stages (the BET SSA of the samples measured after 20

*Corresponding author
Tel.:+39 0817682237; fax:+39 0815936936.
E-mail address: paola.ammendola@irc.cnr.it

carbonation/calcination cycles under ordinary and sound-assisted fluidization conditions is 1.02 and 1.21 m^2 g^{-1}, respectively). However, since the sorbent has such small dimensions, something more happens. In addition to sintering, which causes an intrinsic decline in sorbent surface over repeated cycles, the extreme agglomeration phenomena, due to the natural cohesiveness of the sorbent, contributes to a further reduction of the sorbent surface. Therefore, natural sintering (due to calcination conditions) plus natural agglomeration (due to the fine sorbent particles) lead to a faster carbonation conversion decline under ordinary conditions. On the contrary, when sound is applied, the agglomeration issue is solved and only sintering remains to cause the decline in carbonation conversion. These considerations are confirmed by the SEM images reported in Fig. 9, showing the morphology of CaO derived from $CaCO_3$ after the 20th ordinary and sound-assisted calcination. It is clear that, in both cases, the CaO grains exhibit a certain level of sintering with respect to the fresh sample (Fig. 2b). However, the sample cycled under ordinary conditions are far more sintered than that cycled with the assistance of the acoustic field, which is in line with the observed more prominent deactivation undergone by this sample (Fig. 8).

Notably, the mutlicyclic performances exhibited by the fine CaO particles under sound-assisted fluidization conditions (X_{20} = 0.55, i.e. the carbonation conversion at cycle 20) are better than those reported for coarser limestone (X_{20} = 0.41 [12,13]) and even CaO blends (X_{20} = 0.46 [13,14]) with sintering inhibitors at TCES-CSP operating conditions, thus confirming the findings reported in literature on the positive effect of using small-sized CaO particles on multicycle activity in terms of remarkable limitation of sintering and pore plugging phenomena [12]. In particular, Ortiz et al. [12] explained this evidence referring to both the thickness of the limestone layer formed on the CaO surface, as compared to the size of the pores in the CaO skeleton formed during calcination, and the carbonation kinetics in the fast reaction-controlled stage. Moreover, the results obtained in the

*Corresponding author
Tel.:+39 0817682237; fax:+39 0815936936.
E-mail address: paola.ammendola@irc.cnr.it

present work are slightly better than those obtained for fine natural limestone (< 45 μm) at TCES-CSP operating conditions with TG analysis by other Authors [12,13], thus confirming the ability of sound-assisted fluidization in maximizing the carbonation performances of fine CaO particles [4]. On the contrary, the carbonation performances obtained under ordinary fluidization conditions are worse than those obtained by thermogravimetric analysis [4], thus confirming that thermogravimetry is intrinsically incapable of taking into account all the issues arising from the gas-solid contact and mass/heat transfer efficiency occurring in a fluidized bed reactor.

In analogy to what done for the preliminary fluid-dynamic characterization, the effect of sound frequency and intensity on the CaL performances, in terms of carbonation conversion, has been investigated. Fig. 10 reports the correlation obtained for the carbonation conversion with SPL and frequency, parametric in the cycle number; the values of carbonation conversion obtained without the assistance of any acoustic field have been also reported for comparison. With reference to the effect of SPL, Fig. 10a shows that X_{CaO} monotonically increases with increasing the intensity of the acoustic field. This result, in agreement with the monotonic effect obtained on the fluidization quality (Fig. 4a), is consistent with the enhanced disaggregation mechanism due to the increased strength of the acoustic wave. On the contrary, Fig. 10b shows that the correlation between X_{CaO} and the sound frequency is nonlinear, which is also in agreement with the non-monotonic effect of the sound frequency on the fluidization quality (Fig. 4b). This is in line with the observed existence of an optimum value of sound frequency (120 Hz), at which the propagation of the sound waves inside the bed and, therefore, the disaggregation mechanism is optimized. Notably, even when non-optimal acoustic conditions are applied (i.e. SPL < 150 dB and f ≠ 120 Hz), the carbonation conversion is always larger than that obtainable under ordinary fluidization conditions.

4. Conclusions

*Corresponding author
Tel.:+39 0817682237; fax:+39 0815936936.
E-mail address: paola.ammendola@irc.cnr.it

In this work the possibility to exploit the higher reactivity and mutlicyclic stability of a fine natural limestone (< 50 μm) in a fluidized bed reactor for CaL at TCES-CSP applications has been investigated for the first time. In particular, the acoustic wave perturbation has been proposed to overcome the strong interparticle forces of fine cohesive powders, which leads to agglomeration, channeling and plugging phenomena, thus inhibiting the possibility to uniformly fluidize them.

CaL tests have been performed under ordinary and sound-assisted fluidization conditions in a lab-scale sound-assisted fluidized bed reactor in order to study the influence of the application of high intensity acoustic fields on the carbonation performances of fine CaO particles. The effect of sound parameters (SPL and frequency) has also been highlighted.

It has been found that the application of the acoustic perturbation remarkably enhances the carbonation performances of fine limestone particles under TCES-CSP operating conditions. Indeed, it can hinder the agglomeration phenomena, which negatively affect carbonation from both the gaseous (CO_2) and solid ($CaCO_3$) sides of the reaction, thus enhancing the fluidization quality and providing better gas–solid contact and mass transfer coefficients. Most interestingly, besides increasing the carbonation conversion, the application of the sound results in a remarkable decrease of the deactivation rate. In fact, when such fine sorbent particles are employed under ordinary conditions their strong agglomeration causes a supplementary decrease of sorbent surface in addition to the intrinsic decline over repeated cycles caused by sintering. Therefore, this additional cause of sorbent surface reduction can be avoided when sound is applied, thus resulting in a remarkable limitation of the deactivation rate (which, as in the case of coarser particles, is only due to natural sintering occurring during calcination). The effect of SPL and frequency has also been investigated, showing even further the tight link existing between the gas-solid contact efficiency, i.e. fluidization quality, and the CaL performances. In fact, both SPL and frequency exhibit on the

*Corresponding author
Tel.:+39 0817682237; fax:+39 0815936936.
E-mail address: paola.ammendola@irc.cnr.it

CaL performances the same effect as that obtained from the fluidization experiments, i.e. increasing SPL are advantageous and the same optimum range of frequency has been found.

Since the application of acoustic fields does not involve any material modification, it is rather cheap and could be easily implemented from the technical point of view, it can be foreseen that sound-assisted CaL might be competitive at the industrial level TCES-CSP applications. Pilot-scale experiments and LCA, even though beyond the scope of the present work, will be carried out as next steps of this research activity to further assess the efficiency and feasibility of the proposed technique.

Aknowledgements

This work has been done in the framework of the project SOCRATCES, which has received funding from European Commission by means of Horizon 2020, the EU Framework Programme for Research and Innovation, under Grant Agreement no.727348. Mr. Luciano Cortese is also gratefully acknowledged for SEM analyses.

5. References

[1] C. Ortiz, J.M. Valverde, R. Chacartegui, L.A. Perez-Maqueda, Carbonation of Limestone Derived CaO for Thermochemical Energy Storage: From Kinetics to Process Integration in Concentrating Solar Plants, ACS Sustain. Chem. Eng. 6 (2018) 6404–6417. doi:10.1021/acssuschemeng.8b00199.

[2] E. Karasavvas, K.D. Panopoulos, S. Papadopoulou, S. Voutetakis, Design of an Integrated CSP-Calcium Looping for Uninterrupted Power Production Through Energy Storage, Chem. Eng. Trans. 70 (2018) 2131–2136. doi:10.3303/CET1870356.

[3] P. Salatino, P. Ammendola, P. Bareschino, R. Chirone, R. Solimene, Improving the thermal

*Corresponding author
Tel.:+39 0817682237; fax:+39 0815936936.
E-mail address: paola.ammendola@irc.cnr.it

performance of fluidized beds for concentrated solar power and thermal energy storage, Powder Technol. 290 (2016) 97–101. doi:10.1016/j.powtec.2015.07.036.

[4] J.M. Valverde, F. Raganati, M. a. S. Quintanilla, J.M.P. Ebri, P. Ammendola, R. Chirone, Enhancement of CO2 capture at Ca-looping conditions by high-intensity acoustic fields, Appl. Energy. 111 (2013) 538–549. doi:10.1016/j.apenergy.2013.05.012.

[5] A. Alovisio, R. Chacartegui, C. Ortiz, J.M. Valverde, V. Verda, Optimizing the CSP-Calcium Looping integration for Thermochemical Energy Storage, Energy Convers. Manag. 136 (2017) 85–98. doi:10.1016/j.enconman.2016.12.093.

[6] R. Chacartegui, A. Alovisio, C. Ortiz, J.M. Valverde, V. Verda, J.A. Becerra, Thermochemical energy storage of concentrated solar power by integration of the calcium looping process and a CO 2 power cycle, Appl. Energy. 173 (2016) 589–605. doi:10.1016/j.apenergy.2016.04.053.

[7] C.C. Dean, J. Blamey, N.H. Florin, M.J. Al-Jeboori, P.S. Fennell, The calcium looping cycle for CO2 capture from power generation, cement manufacture and hydrogen production, Chem. Eng. Res. Des. 89 (2011) 836–855. doi:10.1016/j.cherd.2010.10.013.

[8] J. Blamey, E.J. Anthony, J. Wang, P.S. Fennell, The calcium looping cycle for large-scale CO2 capture, Prog. Energy Combust. Sci. 36 (2010) 260–279. doi:10.1016/j.pecs.2009.10.001.

[9] M. Erans, V. Manovic, E.J. Anthony, Calcium looping sorbents for CO2 capture, Appl. Energy. 180 (2016) 722–742. doi:10.1016/j.apenergy.2016.07.074.

[10] B. Dou, Y. Song, Y. Liu, C. Feng, High temperature CO2 capture using calcium oxide

*Corresponding author
Tel.:+39 0817682237; fax:+39 0815936936.
E-mail address: paola.ammendola@irc.cnr.it

sorbent in a fixed-bed reactor, J. Hazard. Mater. 183 (2010) 759–765. doi:10.1016/j.jhazmat.2010.07.091.

[11] A. Perejón, J. Miranda-Pizarro, L.A. Pérez-Maqueda, J.M. Valverde, On the relevant role of solids residence time on their CO 2 capture performance in the Calcium Looping technology, Energy. 113 (2016) 160–171. doi:10.1016/j.energy.2016.07.028.

[12] M. Benitez-Guerrero, B. Sarrion, A. Perejon, P.E. Sanchez-Jimenez, L.A. Perez-Maqueda, J. Manuel Valverde, Large-scale high-temperature solar energy storage using natural minerals, Sol. Energy Mater. Sol. Cells. 168 (2017) 14–21. doi:10.1016/j.solmat.2017.04.013.

[13] C. Ortiz, J.M. Valverde, R. Chacartegui, L.A. Perez-Maqueda, P. Giménez, The Calcium-Looping (CaCO3/CaO) process for thermochemical energy storage in Concentrating Solar Power plants, Renew. Sustain. Energy Rev. 113 (2019) 109252. doi:10.1016/j.rser.2019.109252.

[14] B. Sarrión, A. Perejón, P.E. Sánchez-Jiménez, L.A. Pérez-Maqueda, J.M. Valverde, Role of calcium looping conditions on the performance of natural and synthetic Ca-based materials for energy storage, J. CO2 Util. 28 (2018) 374–384. doi:10.1016/j.jcou.2018.10.018.

[15] M. Benitez-Guerrero, J.M. Valverde, P.E. Sanchez-Jimenez, A. Perejon, L.A. Perez-Maqueda, Calcium-Looping performance of mechanically modified Al2O3-CaO composites for energy storage and CO2 capture, Chem. Eng. J. 334 (2018) 2343–2355. doi:10.1016/j.cej.2017.11.183.

[16] Y. Wang, S. Lin, Y. Suzuki, Limestone Calcination with CO2 Capture (II): Decomposition in CO2/Steam and CO2/N2 Atmospheres, Energy & Fuels. (2008) 2326–2331.

*Corresponding author
Tel.:+39 0817682237; fax:+39 0815936936.
E-mail address: paola.ammendola@irc.cnr.it

[17] J.M. Valverde, P.E. Sanchez-Jimenez, L.A. Perez-Maqueda, Effect of Heat Pretreatment/Recarbonation in the Ca-Looping Process at Realistic Calcination Conditions, Energy & Fuels. 28 (2014) 4062–4067. doi:10.1021/ef5007325.

[18] V. Manovic, E.J. Anthony, Thermal activation of CaO-based sorbent and self-reactivation during CO2 capture looping cycles., Environ. Sci. Technol. 42 (2008) 4170–4. http://www.ncbi.nlm.nih.gov/pubmed/18589983.

[19] P.E. Sánchez-Jiménez, J.M. Valverde, A. Perejón, A. De La Calle, S. Medina, L.A. Pérez-Maqueda, Influence of Ball Milling on CaO Crystal Growth during Limestone and Dolomite Calcination: Effect on CO2 Capture at Calcium Looping Conditions, Cryst. Growth Des. 16 (2016) 7025–7036. doi:10.1021/acs.cgd.6b01228.

[20] A.N. Antzara, A. Arregi, E. Heracleous, A.A. Lemonidou, In-depth evaluation of a ZrO2 promoted CaO-based CO2 sorbent in fluidized bed reactor tests, Chem. Eng. J. 333 (2018) 697–711. doi:10.1016/j.cej.2017.09.192.

[21] S.A. Salaudeen, B. Acharya, A. Dutta, CaO-based CO2 sorbents: A review on screening, enhancement, cyclic stability, regeneration and kinetics modelling, J. CO2 Util. 23 (2018) 179–199. doi:10.1016/j.jcou.2017.11.012.

[22] J. Shabanian, R. Jafari, J. Chaouki, Fluidization of Ultrafine Powders, Int. Rev. Chem. Eng. 4 (2012) 16–50.

[23] F. Raganati, R. Chirone, P. Ammendola, Gas–solid fluidization of cohesive powders, Chem. Eng. Res. Des. 133 (2018) 347–387. doi:10.1016/j.cherd.2018.03.034.

[24] Z. Wei, A Review of Techniques for the Process Intensification of Fluidized Bed Reactors,

*Corresponding author
Tel.:+39 0817682237; fax:+39 0815936936.
E-mail address: paola.ammendola@irc.cnr.it

Chinese J. Chem. Eng. 17 (2009) 688–702.

[25] D. Geldart, Gas fluidization technology, Wiley & Son, Chichester; New York, 1986.

[26] R. Chirone, F. Raganati, P. Ammendola, D. Barletta, P. Lettieri, M. Poletto, A comparison between interparticle forces estimated with direct powder shear testing and with sound assisted fluidization, Powder Technol. 323 (2018) 1–7. doi:10.1016/j.powtec.2017.09.038.

[27] F. Raganati, R. Chirone, P. Ammendola, Effect of Temperature on Fluidization of Geldart's Group A and C Powders: Role of Interparticle Forces, Ind. Eng. Chem. Res. 56 (2017) 12811–12821. doi:10.1021/acs.iecr.7b03270.

[28] F. Raganati, P. Ammendola, R. Chirone, Role of Acoustic Fields in Promoting the Gas-Solid Contact in a Fluidized Bed of Fine Particles, KONA Powder Part. J. 32 (2015) 23–40. doi:10.14356/kona.2015006.

[29] J.P.K. Seville, C.D. Willett, P.C. Knight, Interparticle forces in fluidisation: A review, Powder Technol. 113 (2000) 261–268. doi:10.1016/S0032-5910(00)00309-0.

[30] C.H. Nam, R. Pfeffer, R.N. Dave, S. Sundaresan, Aerated vibrofluidization of silica nanoparticles, AIChE J. 50 (2004) 1776–1785. doi:10.1002/aic.10237.

[31] J. Yang, T. Zhou, L. Song, Agglomerating vibro-fluidization behavior of nano-particles, Adv. Powder Technol. 20 (2009) 158–163. doi:10.1016/j.apt.2008.06.002.

[32] P. Zeng, T. Zhou, J. Yang, Behavior of mixtures of nano-particles in magnetically assisted fluidized bed, Chem. Eng. Process. Process Intensif. 47 (2008) 101–108. doi:10.1016/j.cep.2007.08.009.

[33] Q. Yu, R.N. Dave, C. Zhu, J.A. Quevedo, R. Pfeffer, Enhanced Fluidization of Nanoparticles

*Corresponding author
Tel.:+39 0817682237; fax:+39 0815936936.
E-mail address: paola.ammendola@irc.cnr.it

in an Oscillating Magnetic Field, AIChE J. 51 (2005) 1971–1979. doi:10.1002/aic.10479.

[34] D. Lepek, J.M. Valverde, R. Pfeffer, R.N. Dave, Enhanced nanofluidization by alternating electric fields, AIChE J. 56 (2010) 54–65. doi:10.1002/aic.11954.

[35] J.M. Valverde, M.J. Espin, M.A.S. Quintanilla, A. Castellanos, Electrofluidized bed of silica nanoparticles, J. Electrostat. 67 (2009) 439–444. doi:10.1016/j.elstat.2009.01.021.

[36] H. Nakamura, S. Watano, Fundamental particle fluidization behavior and handling of nano-particles in a rotating fluidized bed, Powder Technol. 183 (2008) 324–332. doi:10.1016/j.powtec.2008.01.007.

[37] G.-H. Qian, I. Bágyi, I.W. Burdick, R. Pfeffer, H. Shaw, J.G. Stevens, Gas–solid fluidization in a centrifugal field, AIChE J. 47 (2001) 1022–1034. doi:10.1002/aic.690470509.

[38] S. Matsuda, H. Hatano, T. Muramoto, A. Tsutsumi, Modeling for Size Reduction of Agglomerates in Nanoparticle Fluidization, AIChE J. 50 (2004) 2763–2771. doi:10.1002/aic.10258.

[39] J. Quevedo, R. Pfeffer, Y. Shen, R. Dave, Fluidization of Nanoagglomerates in a Rotating Fluidized Bed, AIChE J. 52 (2006) 2401–2412. doi:10.1002/aic.

[40] J.A. Quevedo, A. Omosebi, R. Pfeffer, Fluidization enhancement of agglomerates of metal oxide nanopowders by microjets, AIChE J. 56 (2010) 1456–1468. doi:10.1002/aic.12075.

[41] R. Pfeffer, J.A. Quevedo, J. Flesch, Fluidized Bed Systems And Methods Including Micro-Jet Flow, United States Patent Application US20080179433 A1, 2008.

[42] A. Akhavan, J.R. Van Ommen, J. Nijenhuis, X.S. Wang, M.O. Coppens, M.J. Rhodes, Improved drying in a pulsation-assisted fluidized bed, Ind. Eng. Chem. Res. 48 (2009) 302–

*Corresponding author
Tel.:+39 0817682237; fax:+39 0815936936.
E-mail address: paola.ammendola@irc.cnr.it

309. doi:10.1021/ie800458h.

[43] X.S. Wang, M.J. Rhodes, Using pulsed flow to overcome defluidization, Chem. Eng. Sci. 60 (2005) 5177–5181. doi:10.1016/j.ces.2005.04.016.

[44] A. Akhavan, F. Rahman, X.S. Wang, M.J. Rhodes, Assisted fluidization of nanoparticles through gas-phase pulsation, in: CHEMECA 2007, Melbourne (Australia), 2007.

[45] H. Duan, X. Liang, T. Zhou, J. Wang, W. Tang, Fluidization of mixed SiO2 and ZnO nanoparticles by adding coarse particles, Powder Technol. 267 (2014) 315–321. doi:10.1016/j.powtec.2014.07.045.

[46] L. Song, T. Zhou, J. Yang, Fluidization behavior of nano-particles by adding coarse particles, Adv. Powder Technol. 20 (2009) 366–370. doi:10.1016/j.apt.2009.02.010.

[47] J.M. Valverde Millán, Fluidization of Fine Powders, Springer Netherlands, Dordrecht, 2013. doi:10.1007/978-94-007-5587-1.

[48] M.A.S. Quintanilla, A. Castellanos, J.M. Valverde, Correlation between bulk stresses and interparticle contact forces in fine powders, Phys. Rev. E. 64 (2001) 031301. doi:10.1103/PhysRevE.64.031301.

[49] P. Ammendola, F. Raganati, R. Chirone, Effect of operating conditions on the CO2 recovery from a fine activated carbon by means of TSA in a fluidized bed assisted by acoustic fields, Fuel Process. Technol. 134 (2015) 494–501. doi:10.1016/j.fuproc.2015.03.010.

[50] A. Viscusi, P. Ammendola, A. Astarita, F. Raganati, F. Scherillo, A. Squillace, R. Chirone, L. Carrino, Aluminum foam made via a new method based on cold gas dynamic sprayed powders mixed through sound assisted fluidization technique, J. Mater. Process. Technol.

*Corresponding author
Tel.:+39 0817682237; fax:+39 0815936936.
E-mail address: paola.ammendola@irc.cnr.it

231 (2016) 265–276. doi:10.1016/j.jmatprotec.2015.12.030.

[51] F. Raganati, F. Scherillo, A. Squillace, R. Chirone, P. Ammendola, Improvement of the Manufacturing Process of Tungsten Carbide–Cobalt Hard Metals by the Application of Sound Assisted Fluidization for the Mixing of the Powders, Ind. Eng. Chem. Res. 57 (2018) 414–424. doi:10.1021/acs.iecr.7b04627.

[52] R. Chirone, L. Massimilla, S. Russo, Bubble-Free Fluidization Of A Cohesive Powder In An Acoustic Field, Chem. Eng. Sci. 48 (1993) 41–52.

[53] P. Russo, R. Chirone, L. Massimilla, S. Russo, The influence of the frequency of acoustic waves on sound-assisted fluidization of beds of fine particles, Powder Technol. 82 (1995) 219–230. doi:10.1016/0032-5910(94)02931-D.

[54] J. Ahrens, S. Spors, Sound field reproduction using planar and linear arrays of loudspeakers, IEEE Trans. Audio, Speech Lang. Process. (2010). doi:10.1109/TASL.2010.2041106.

[55] D.B. Ward, T.D. Abhayapala, Reproduction of a plane-wave sound field using an array of loudspeakers, IEEE Trans. Speech Audio Process. (2001). doi:10.1109/89.943347.

[56] C.Y. Wen, Y.H. Yu, A generalized method for predicting the minimum fluidization velocity, AIChE J. 12 (1966) 610–612. doi:10.1002/aic.690120343.

[57] P.E. Sánchez Jiménez, A. Perejón, M. Benítez Guerrero, J.M. Valverde, C. Ortiz, L.A. Pérez Maqueda, High-performance and low-cost macroporous calcium oxide based materials for thermochemical energy storage in concentrated solar power plants, Appl. Energy. 235 (2019) 543–552. doi:10.1016/j.apenergy.2018.10.131.

[58] J.S. Dennis, R. Pacciani, The rate and extent of uptake of CO2 by a synthetic, CaO-

*Corresponding author
Tel.:+39 0817682237; fax:+39 0815936936.
E-mail address: paola.ammendola@irc.cnr.it

containing sorbent, Chem. Eng. Sci. 64 (2009) 2147–2157. doi:10.1016/j.ces.2009.01.051.

[59] J.F. Davidson, J.S. Dennis, A.N. Hayhurst, How Does the Concentration of CO2 Affect Its Uptake by a Synthetic Ca-Based Solid Sorbent ?, AIChE J. 54 (2008) 12–15. doi:10.1002/aic.

[60] W. Liu, J.S. Dennis, D.S. Sultan, S.A.T. Redfern, S.A. Scott, An investigation of the kinetics of CO 2 uptake by a synthetic calcium based sorbent, Chem. Eng. Sci. 69 (2012) 644–658. doi:10.1016/j.ces.2011.11.036.

[61] M.H. Sedghkerdar, E. Mostafavi, N. Mahinpey, Investigation of the Kinetics of Carbonation Reaction with Cao-Based Sorbents Using Experiments and Aspen Plus Simulation, Chem. Eng. Commun. 202 (2015) 746–755. doi:10.1080/00986445.2013.871709.

[62] F. Raganati, M. Alfe, V. Gargiulo, R. Chirone, P. Ammendola, Kinetic study and breakthrough analysis of the hybrid physical/chemical CO2 adsorption/desorption behavior of a magnetite-based sorbent, Chem. Eng. J. 372 (2019) 526–535. doi:10.1016/j.cej.2019.04.165.

[63] F. Raganati, M. Alfe, V. Gargiulo, R. Chirone, P. Ammendola, Isotherms and thermodynamics of CO2 adsorption on a novel carbon-magnetite composite sorbent, Chem. Eng. Res. Des. 134 (2018) 540–552. doi:10.1016/j.cherd.2018.04.037.

[64] V. Gargiulo, M. Alfè, P. Ammendola, F. Raganati, R. Chirone, CO2 sorption on surface-modified carbonaceous support: Probing the influence of the carbon black microporosity and surface polarity, Appl. Surf. Sci. 360 (2016) 329–337. doi:10.1016/j.apsusc.2015.11.026.

[65] V. Gargiulo, M. Alfè, F. Raganati, L. Lisi, R. Chirone, P. Ammendola, BTC-based metal-

*Corresponding author
Tel.:+39 0817682237; fax:+39 0815936936.
E-mail address: paola.ammendola@irc.cnr.it

organic frameworks: Correlation between relevant structural features and CO2 adsorption performances, Fuel. 222 (2018) 319–326. doi:10.1016/j.fuel.2018.02.093.

[66] M. Kavosh, K. Patchigolla, E.J. Anthony, J.E. Oakey, Carbonation performance of lime for cyclic CO2 capture following limestone calcination in steam/CO2 atmosphere, Appl. Energy. 131 (2014) 499–507. doi:10.1016/j.apenergy.2014.05.020.

[67] J. Yin, C. Qin, B. Feng, L. Ge, C. Luo, W. Liu, H. An, Calcium Looping for CO2 Capture at a Constant High Temperature, Energy & Fuels. 28 (2014) 307–318. doi:10.1021/ef401399c.

[68] B. Formisani, R. Girimonte, G. Pataro, The influence of operating temperature on the dense phase properties of bubbling fluidized beds of solids, Powder Technol. 125 (2002) 28–38. doi:10.1016/S0032-5910(01)00494-6.

[69] F. Raganati, P. Ammendola, R. Chirone, On improving the CO2 recovery efficiency of a conventional TSA process in a sound assisted fluidized bed by separating heating and purging, Sep. Purif. Technol. 167 (2016) 24–31. doi:10.1016/j.seppur.2016.05.001.

[70] F. Raganati, P. Ammendola, R. Chirone, Effect of acoustic field on CO2 desorption in a fluidized bed of fine activated carbon, Particuology. 23 (2015) 8–15. doi:10.1016/j.partic.2015.02.001.

*Corresponding author
Tel.:+39 0817682237; fax:+39 0815936936.
E-mail address: paola.ammendola@irc.cnr.it

Figure captions

Fig. 1. Experimental apparatus: (1) N_2 cylinder; (2) CO_2 cylinder (3) N_2 flow meter; (4) CO_2 flow meter; (5) controller; (6) 40mm ID fluidization column; (7) wind-box; (8) microphone; (9) sound wave guide; (10) loudspeaker; (11) pressure transducer; (12) thermocouple; (13) temperature controller; (14) heating jacket; (15) filter; (16) CO_2 analyzer; (17) stack.

Fig. 2. Granulometric size distribution (a) and SEM image (b) of the natural limestone.

Fig. 3. Pressure drops curves of the natural limestone obtained under ordinary and sound assisted fluidization conditions at 25 °C.

Fig. 4. Minimum fluidization velocity and fluidizing agglomerate size of the natural limestone as functions of SPL at fixed frequency (120 Hz) (a) and as functions of frequency at fixed SPL (150 dB) (b). Temperature = 25 °C.

Fig. 5. a) Pressure drops curves of the natural limestone obtained under sound assisted fluidization conditions (150dB – 120Hz) at different temperatures; b) Minimum fluidization velocity and fluidizing agglomerate size of the natural limestone as functions of temperature. SPL = 150dB; f = 120Hz.

Fig. 6. Pictures of the fluidized bed taken during ordinary (a) and sound-assisted (150dB – 120 Hz) (b) fluidization tests. Temperature = 850 °C.

Fig. 7. a) CO_2 concentration measured in the effluent gas from the fluidized bed during carbonation for an ordinary fluidization test, a sound-assisted fluidization test and for a test in which the sound was switched on at t = t*; b) Carbonation conversion as a function of time obtained under ordinary and sound-assisted conditions during the first cycle. Inlet flow rate: 115

*Corresponding author
Tel.:+39 0817682237; fax:+39 0815936936.
E-mail address: paola.ammendola@irc.cnr.it

NLh^{-1}; Carbonation: T = 850 °C; 70%vol. of CO_2 in N_2. Calcination: T = 750 °C; 100%vol. N_2.

Fig. 8. Carbonation conversion as a function of cycle number and deactivation fit curve obtained under ordinary and sound assisted-fluidization conditions. Inlet flow rate: 115 NLh^{-1}; Carbonation: T = 850 °C; 70%vol. of CO_2 in N_2. Calcination: T = 750 °C; 100%vol. N_2.

Fig. 9. SEM images at different magnification of the limestone subjected to ordinary (a, b) and sound assisted (150 dB – 120 Hz) (c, d) CaL cycles after calcination at the 20th cycles.

Fig. 10. Carbonation conversion as a function of (a) SPL, at a fixed sound frequency (120 Hz), and (b) frequency, at a fixed SPL (150 dB).

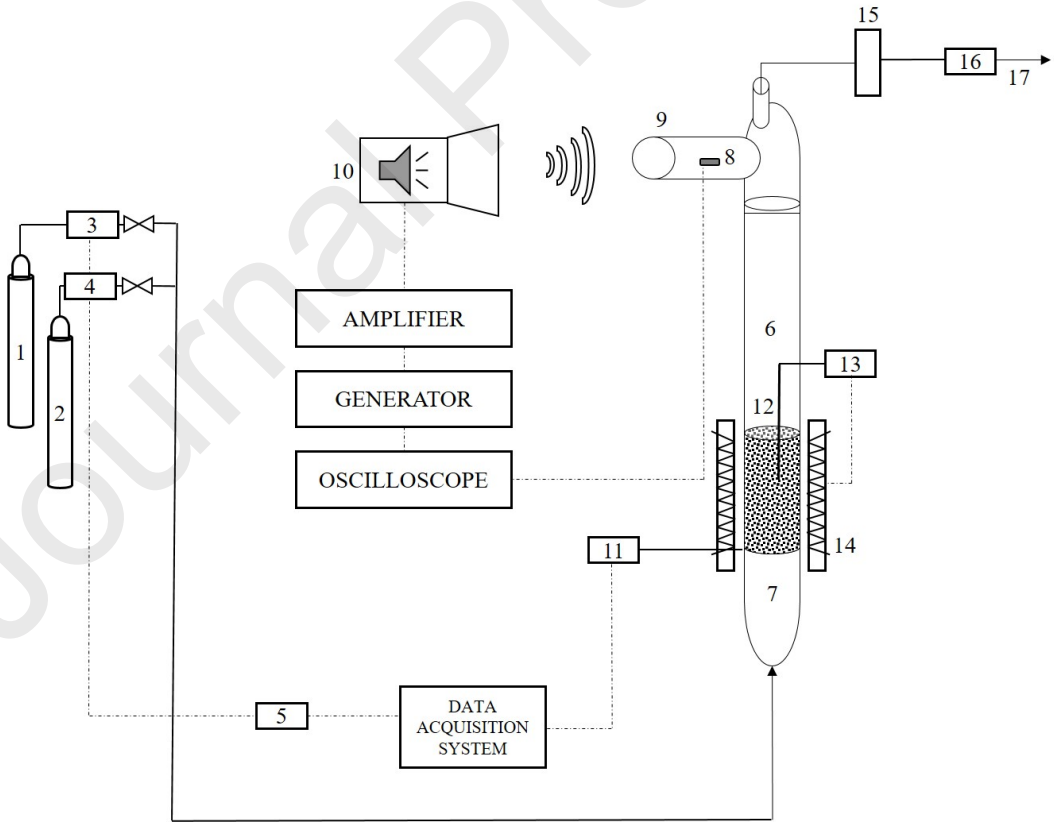

*Corresponding author
Tel.:+39 0817682237; fax:+39 0815936936.
E-mail address: paola.ammendola@irc.cnr.it

Figure 1. Experimental apparatus: (1) N_2 cylinder; (2) CO_2 cylinder (3) N_2 flow meter; (4) CO_2 flow meter; (5) controller; (6) 40mm ID fluidization column; (7) wind-box; (8) microphone; (9) sound wave guide; (10) loudspeaker; (11) pressure transducer; (12) thermocouple; (13) temperature controller; (14) heating jacket; (15) filter; (16) CO_2 analyzer; (17) stack.

*Corresponding author

Tel.:+39 0817682237; fax:+39 0815936936.

E-mail address: paola.ammendola@irc.cnr.it

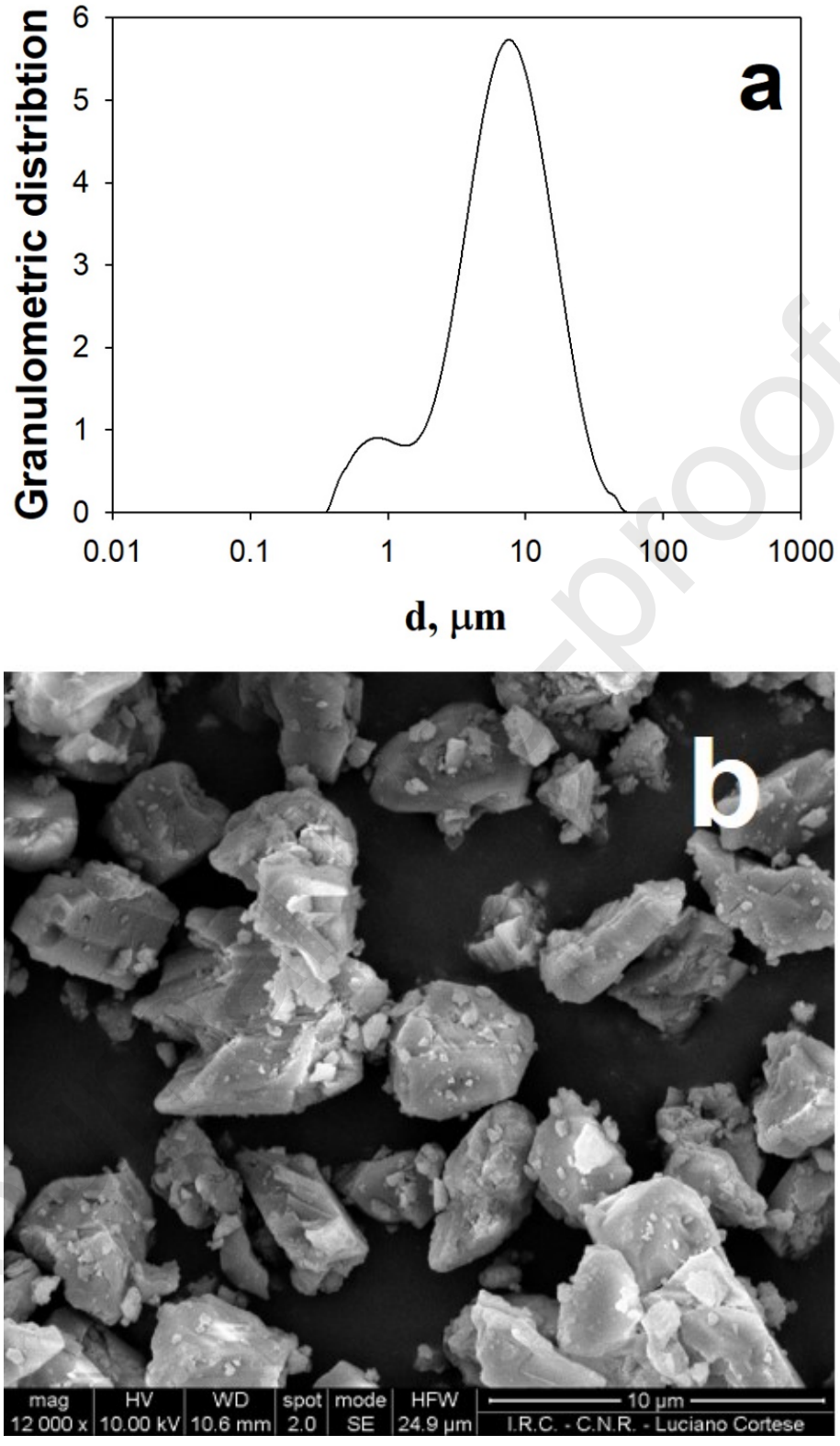

Figure 2. Granulometric size distribution (a) and SEM image (b) of the natural limestone.

*Corresponding author

Tel.:+39 0817682237; fax:+39 0815936936.

E-mail address: paola.ammendola@irc.cnr.it

*Corresponding author

Tel.:+39 0817682237; fax:+39 0815936936.

E-mail address: paola.ammendola@irc.cnr.it

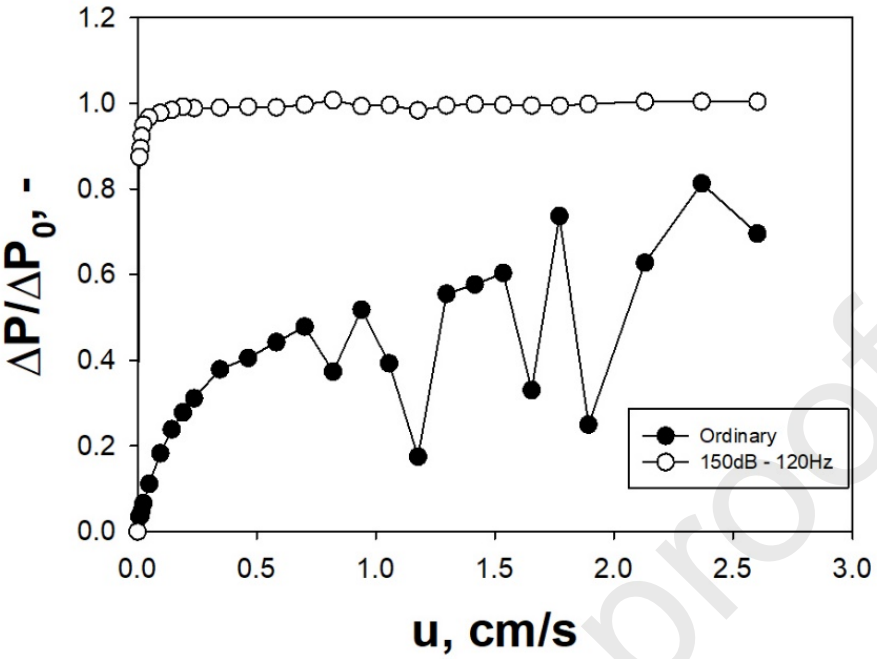

Figure 3. Pressure drops curves of the natural limestone obtained under ordinary and sound assisted fluidization conditions at 25 °C.

*Corresponding author

Tel.:+39 0817682237; fax:+39 0815936936.

E-mail address: paola.ammendola@irc.cnr.it

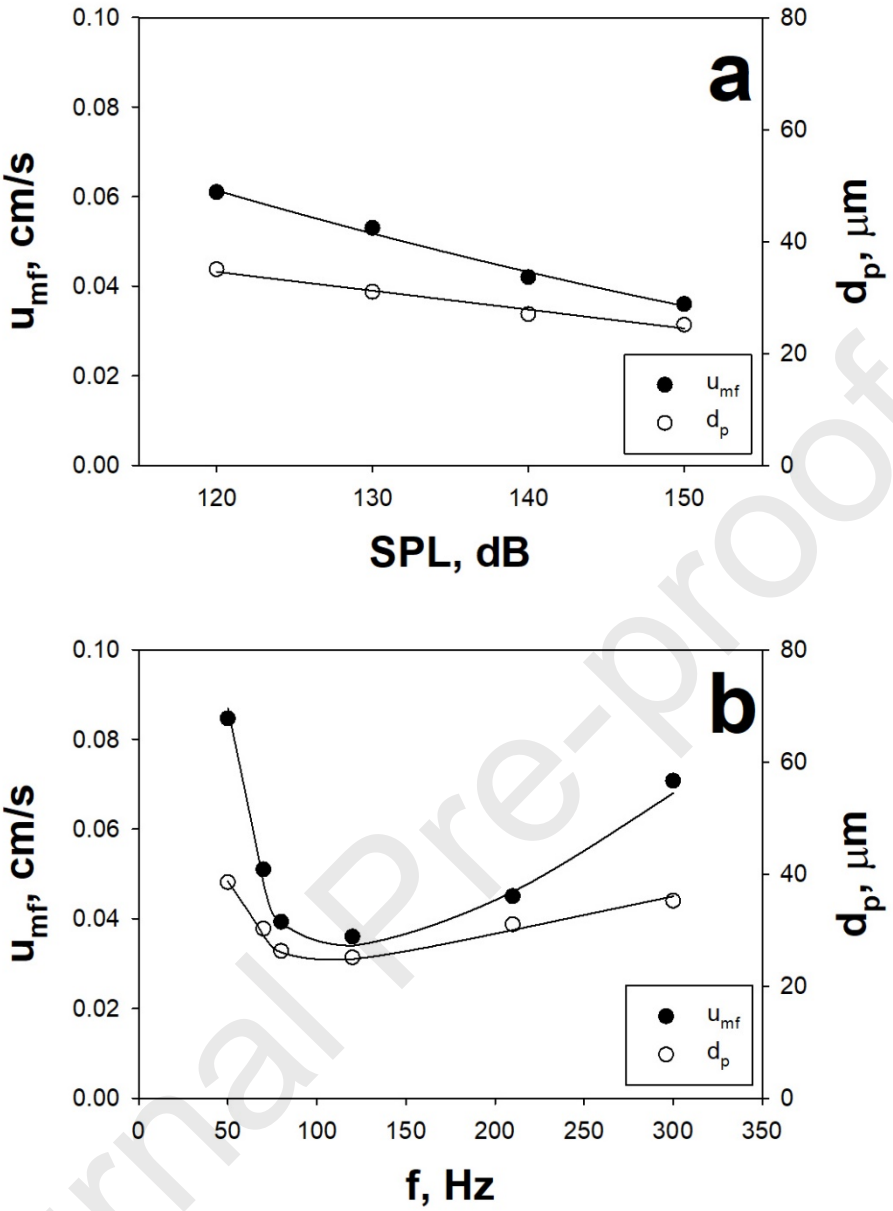

Figure 4. Minimum fluidization velocity and fluidizing agglomerate size of the natural limestone as functions of SPL at fixed frequency (120 Hz) (a) and as functions of frequency at fixed SPL (150 dB) (b). Temperature = 25 °C.

*Corresponding author

Tel.:+39 0817682237; fax:+39 0815936936.

E-mail address: paola.ammendola@irc.cnr.it

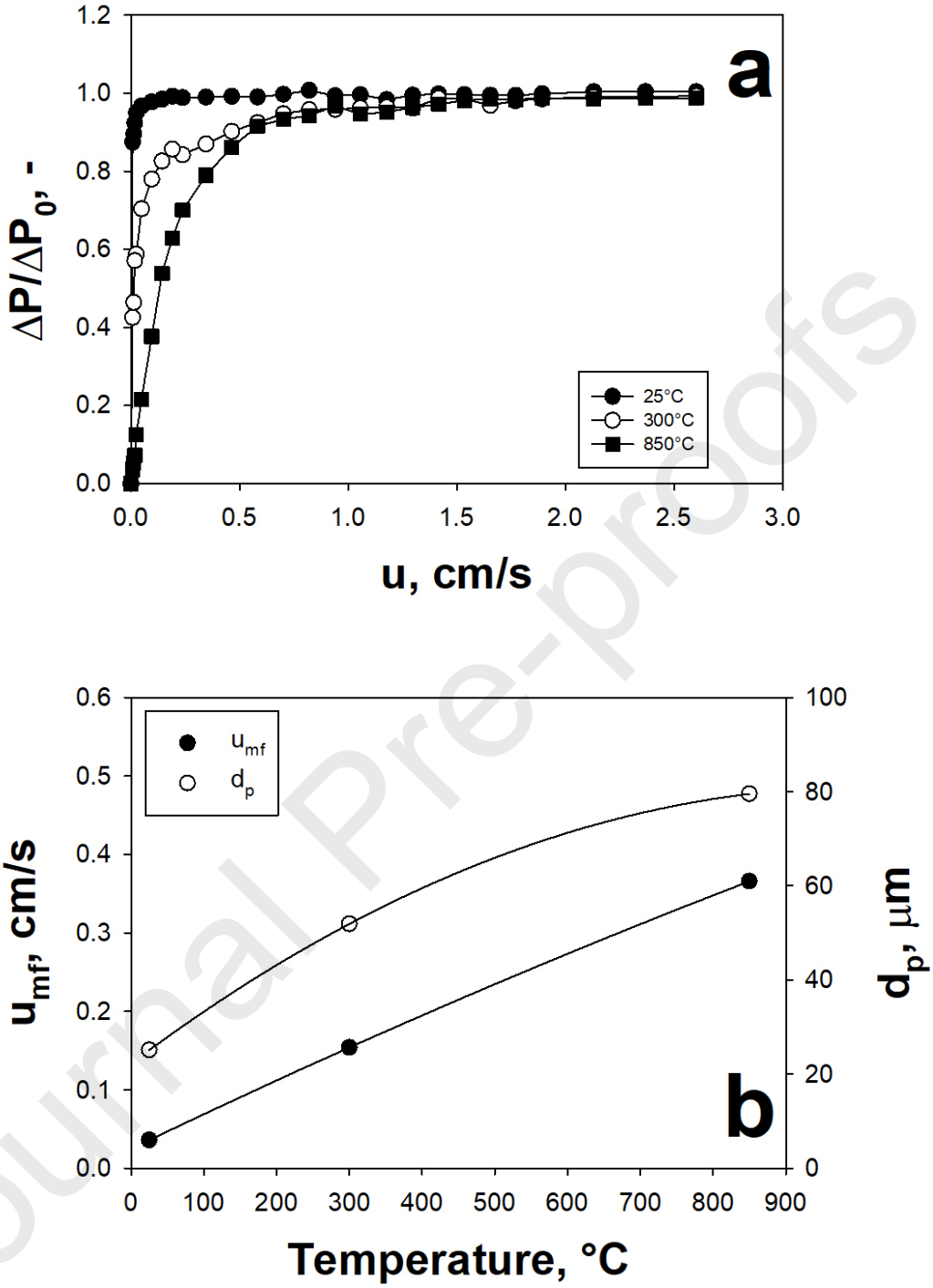

Figure 5. a) Pressure drops curves of the natural limestone obtained under sound assisted fluidization conditions (150dB – 120Hz) at different temperatures; b) Minimum fluidization velocity and fluidizing agglomerate size of the natural limestone as functions of temperature. SPL = 150dB; f = 120Hz.

*Corresponding author

Tel.:+39 0817682237; fax:+39 0815936936.

E-mail address: paola.ammendola@irc.cnr.it

*Corresponding author

Tel.:+39 0817682237; fax:+39 0815936936.

E-mail address: paola.ammendola@irc.cnr.it

Figure 6. Pictures of the fluidized bed taken during ordinary (a) and sound-assisted (150dB – 120 Hz) (b) fluidization tests. Temperature = 850 °C.

*Corresponding author

Tel.:+39 0817682237; fax:+39 0815936936.

E-mail address: paola.ammendola@irc.cnr.it

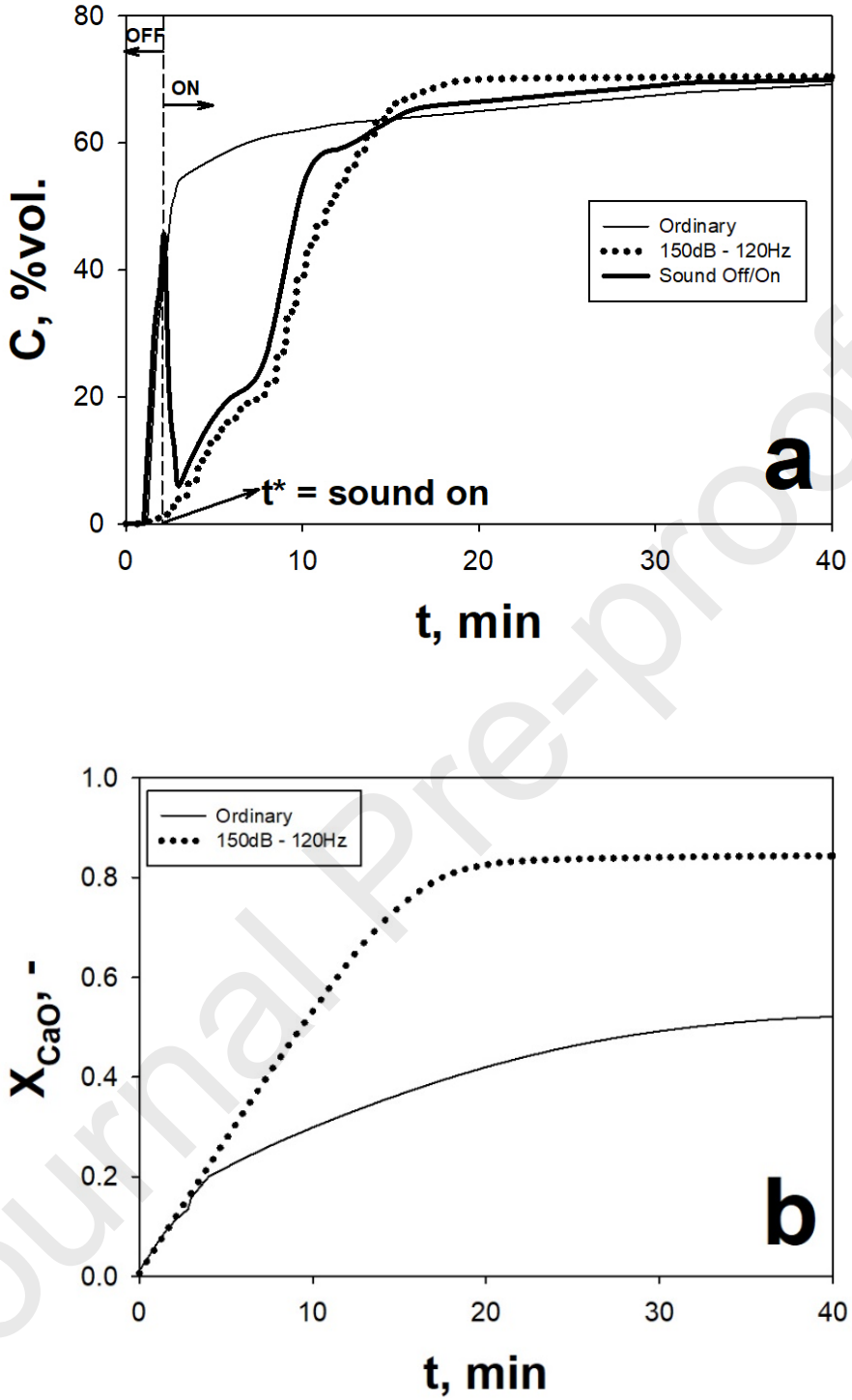

Figure 7. a) CO_2 concentration measured in the effluent gas from the fluidized bed during carbonation for an ordinary fluidization test, a sound-assisted fluidization test and for a test in which the sound was switched on at t = t*; b) Carbonation conversion as a function of time obtained under ordinary and sound-assisted conditions during the first cycle. Inlet flow rate:

*Corresponding author

Tel.:+39 0817682237; fax:+39 0815936936.

E-mail address: paola.ammendola@irc.cnr.it

115 NLh^{-1}; Carbonation: T = 850 °C; 70%vol. of CO_2 in N_2. Calcination: T = 750 °C; 100%vol. N_2.

*Corresponding author

Tel.:+39 0817682237; fax:+39 0815936936.

E-mail address: paola.ammendola@irc.cnr.it

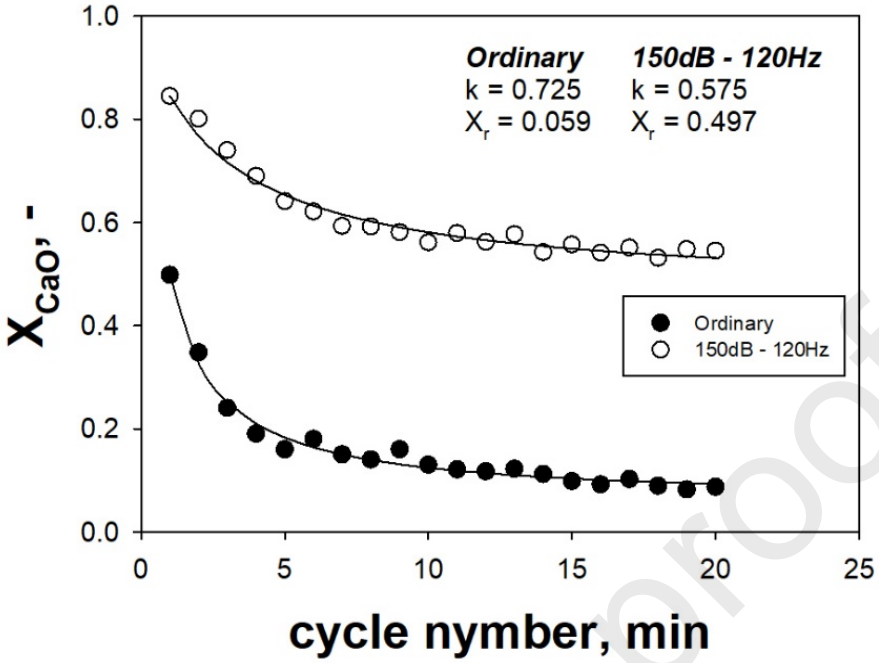

Figure 8. Carbonation conversion as a function of cycle number and deactivation fit curve obtained under ordinary and sound assisted-fluidization conditions. Inlet flow rate: 115 NLh^{-1}; Carbonation: T = 850 °C; 70%vol. of CO_2 in N_2. Calcination: T = 750 °C; 100%vol. N_2.

*Corresponding author

Tel.:+39 0817682237; fax:+39 0815936936.

E-mail address: paola.ammendola@irc.cnr.it

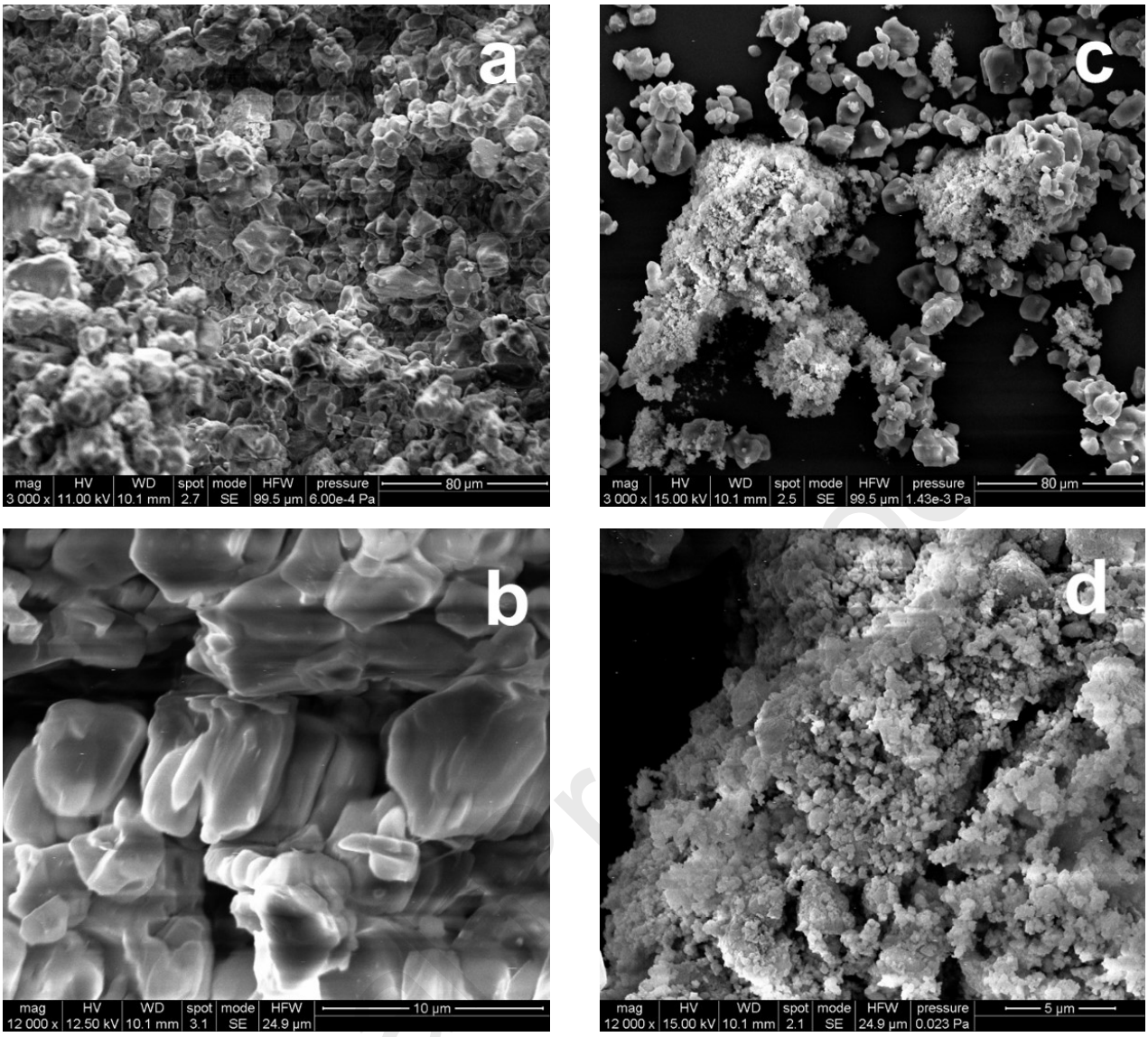

Figure 9. SEM images at different magnification of the limestone subjected to ordinary (a, b) and sound assisted (150 dB – 120 Hz) (c, d) CaL cycles after calcination at the 20th cycles.

*Corresponding author

Tel.:+39 0817682237; fax:+39 0815936936.

E-mail address: paola.ammendola@irc.cnr.it

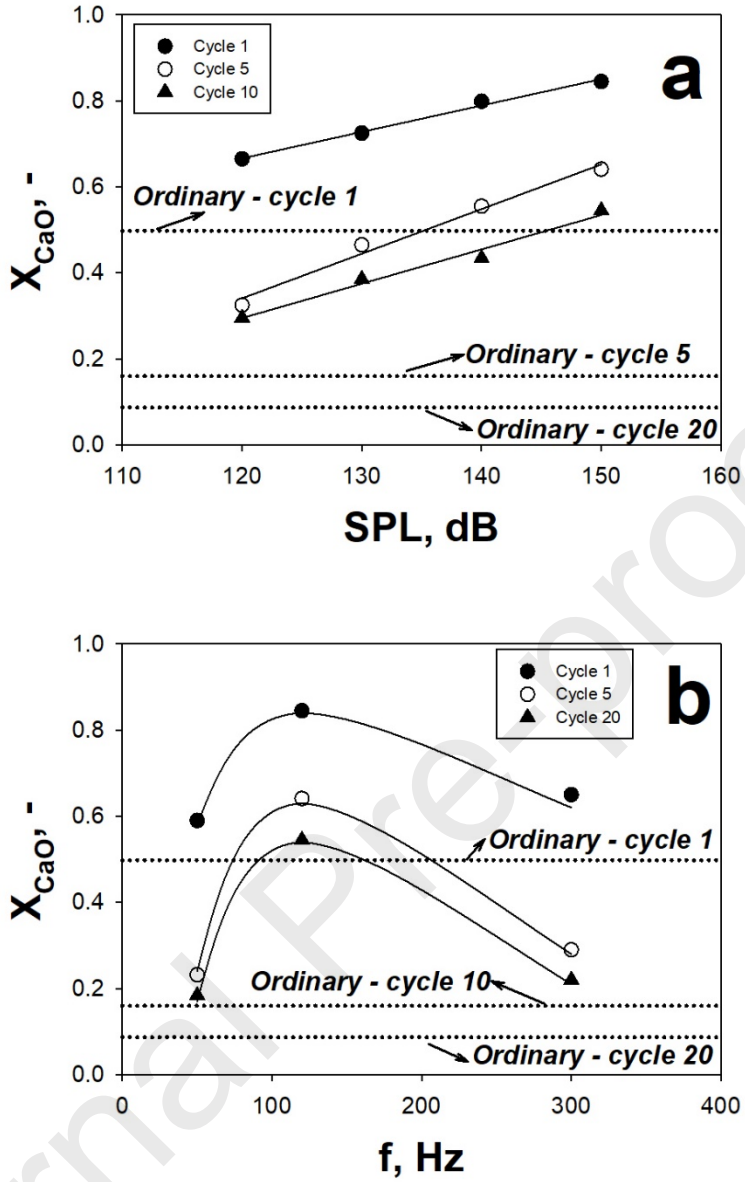

Figure 10. Carbonation conversion as a function of (a) SPL, at a fixed sound frequency (120 Hz), and (b) frequency, at a fixed SPL (150 dB).

The Authors, whose names are listed immediately below, certify that:

*Corresponding author

Tel.:+39 0817682237; fax:+39 0815936936.

E-mail address: paola.ammendola@irc.cnr.it

- they have NO affiliations with or involvement in any organization or entity with any financial interest, or non-financial interest in the subject matter or materials discussed in this manuscript
- all of the sources of funding for the work described in this publication are acknowledged

Federica Raganati

Riccardo Chirone

Paola Ammendola

Highlights

1. Fine limestone has been tested for TCES-CSP for its superior mutlicyclic stability
2. TCES CaL of fine limestone has been performed in a lab-scale fluidized bed rig
3. Acoustic perturbation has been used to overcome the strong interparticle forces
4. The sound application enhances the carbonation performances of fine limestone
5. The sound application results in a strong reduction of the sorbent deactivation

*Corresponding author

Tel.:+39 0817682237; fax:+39 0815936936.

E-mail address: paola.ammendola@irc.cnr.it